

Cyclic AMP Modulation of Ion Transport Across Frog Retinal Pigment Epithelium

Measurements in the Short-Circuit State

SHELDON MILLER and DEBORA FARBER

From the School of Optometry, University of California, Berkeley, California 94720, and Jules Stein Eye Institute, University of California School of Medicine, Los Angeles, California 90024

ABSTRACT In the frog retinal pigment epithelium (RPE), the cellular levels of cyclic AMP (cAMP) were measured in control conditions and after treatment with substances that are known to inhibit phosphodiesterase (PDE) activity (isobutyl-1-methylxanthine, SQ65442) or stimulate adenylate cyclase activity (forskolin). The cAMP levels were elevated by a factor of 5–7 compared with the controls in PDE-treated tissues and by a factor of 18 in forskolin-treated tissues. The exogenous application of cAMP (1 mM), PDE inhibitors (0.5 mM), or forskolin (0.1 mM) all produced similar changes in epithelial electrical parameters, such as transepithelial potential (TEP) and resistance (R_t), as well as changes in active ion transport. Adding 1 mM cAMP to the solution bathing the apical membrane transiently increased the short-circuit current (SCC) and the TEP (apical side positive) and decreased R_t . Microelectrode experiments showed that the elevation in TEP is due mainly to a depolarization of the basal membrane followed by, and perhaps also accompanied by, a smaller hyperpolarization of the apical membrane. The ratio of the apical to the basolateral membrane resistance increased in the presence of cAMP, and this increase, coupled with the decrease in R_t and the basolateral membrane depolarization, is consistent with a conductance increase at the basolateral membrane. Radioactive tracer experiments showed that cAMP increased the active secretion of Na (choroid to retina) and the active absorption of K (retina to choroid). Cyclic AMP also abolished the active absorption of Cl across the RPE. In sum, elevated cellular levels of cAMP affect active and passive transport mechanisms at the apical and basolateral membranes of the bullfrog RPE.

INTRODUCTION

The pigment epithelium (PE) lies at the back of the vertebrate eye and separates the choroidal blood supply and the neural retina. The apical membrane of this epithelium has a close anatomical relationship to the photoreceptor outer segments (Nilsson, 1964; Steinberg and Wood, 1979), which suggests that alterations

Address reprint requests to Dr. Sheldon Miller, 360 Minor Hall, University of California, Berkeley, CA 94720.

in epithelial transport may modulate the chemical milieu of the extracellular (or subretinal) space separating the PE and the photoreceptors. It has been shown that alterations in the chemical milieu of the subretinal space can affect the physiological activity of the PE and the photoreceptors (Oakley, 1977; Miller and Steinberg, 1979; Steinberg et al., 1980; Capovilla et al., 1980).

Starting from the work of Orloff and Handler (1962) on toad bladder, it has been shown in a wide variety of epithelia (Rasmussen, 1981) that changes in cyclic AMP (cAMP) metabolism can significantly alter the transepithelial movement of electrolyte and water. This kind of control mechanism could be of great functional significance for the PE because of its role in maintaining the chemical milieu of the subretinal space (the extracellular space between the photoreceptors and the PE) and because there are a host of retinal and pigment epithelial pathologies that lead to the accumulation of fluid in the subretinal space and the subsequent disruption of vision (Gass, 1977; Zauberman, 1979).

Over the last decade, an extensive amount of information has accumulated concerning the role of cyclic nucleotides in the vertebrate retina. Much of this work has focused on the possible role of cyclic GMP in rod photoreceptor physiology (W. H. Miller, 1981). Recently, however, an increasingly important role has also emerged for cAMP in: (a) the inner retina (Brown and Makman, 1972; Van Buskirk and Dowling, 1981), (b) the cone photoreceptors (Farber et al., 1981), (c) retinomotor movements of photoreceptors and PE (Burnside et al., 1982), and (d) photoreceptor disk shedding (Besharse et al., 1982).

In this paper we show that the elevation of cAMP levels in the PE cells can significantly alter the mechanisms of active and passive transport that are located on the apical and basal membranes of the epithelium (Miller and Steinberg, 1977a, b, 1979, 1982; Miller et al., 1978; Oakley et al., 1978; Steinberg and Miller, 1979). In the companion paper (Hughes et al., 1984), we show that there is an active transport-generated absorption of fluid across the PE that is inhibited by elevating cellular cAMP. Some of this work has been previously reported in abstract form (Miller and Farber, 1981; Miller, 1982) and summarized in a short report (Miller et al., 1982).

METHODS

These studies were performed on the isolated retinal pigment epithelium (RPE)-choroid of the bullfrog, *Rana catesbeiana*. The RPE consists of a single layer of cuboidal cells. The basal surface of the RPE faces the choroid, which is ~130 μm thick and consists mainly of blood vessels and melanocytes dispersed in a fibrous stroma. Individual RPE cells measure ~15 μm in width and depth (Porter and Yamada, 1960; Nilsson, 1964; Steinberg, 1973). The junctional complexes connecting these cells in frogs differ from those of other species by being located not at the cellular apices but at least halfway down the lateral surfaces of each cell (Porter and Yamada, 1960; Hudspeth and Yee, 1973). The apical surface of the RPE faces the sensory retina and consists of villous processes that are 60–90 μm long. These processes are closely apposed to the photoreceptors and extend all the way down to their inner segments (Nilsson, 1964).

The bullfrogs were obtained from Central Valley Biologicals (Clovis, CA) and kept from several days to several weeks in running tap water at 19°C, on an alternating 12-h cycle of light and darkness. Pieces of PE-choroid, 6.5 mm square, were isolated from dark-adapted eyes and mounted in a Lucite chamber so that the surface of the choroid

and the apical surface of the PE were immersed in separate 1.8-ml baths whose compositions could be separately controlled. The chamber design and the techniques used for dissecting the tissue and mounting it between two Lucite plates were identical to those used previously (Miller and Steinberg, 1977*a, b*).

The composition of the control bathing solution was (in mM): 82.5 NaCl, 27.5 NaHCO₃, 2.0 KCl, 1.0 MgCl₂, 1.8 CaCl₂, 10.0 glucose; it was gassed with 95% O₂/5% CO₂ to a pH of 7.4 ± 0.1. The osmolality of this solution was 227 mosmol. In some experiments, cyclic nucleotides and/or phosphodiesterase (PDE) inhibitors were added to the solutions bathing the apical and/or basal membranes. The quantities added were: 1 mM cAMP or dibutyryl cAMP (dbcAMP) (from Sigma Chemical Co., St. Louis, MO), 0.5 mM isobutyl-1-methylxanthine (IBMX) (Sigma Chemical Co.), and 1 mM SQ65442 (from E. R. Squibb and Sons, Princeton, NJ). In some experiments, the SQ65442 was dissolved in 0.4% dimethylsulfoxide (DMSO).

Two pairs of agar-Ringer bridges on each side of the tissue were used to monitor the transepithelial potential (TEP) and to pass current both for short-circuiting and for measuring the transepithelial resistance (R_t). The short-circuit current (SCC) was monitored continuously on a pen recorder. Readings of TEP were obtained hourly by briefly interrupting the short circuit, and R_t was also obtained at the same time by passing 1- μ A pulses transepithelially and recording changes in TEP.

For the determination of the transepithelial unidirectional fluxes, radioisotopes were added either to the basal solution or to the apical solution. The fluxes, apical → basal (retina → choroid) or basal → apical (choroid → retina), were then measured by sampling the "cold" solution on the opposite side of the tissue every 20 min. The sample size was 100 μ l, and it was replaced with an equal amount of "cold" solution. Samples were assayed by conventional counting techniques, using a Beckman LS-7500 liquid scintillation counter (Beckman Instruments, Inc., Mountain View, CA). The unidirectional fluxes were calculated in nanomoles per square centimeter per hour from the rate of tracer appearance on the "cold" side and the specific activity of the "hot" side; the area refers to the geometrical area of the tissue exposed to the two bathing solutions and was 0.07 cm². The fluid in each chamber was stirred and oxygenated by a stream of water-saturated gas bubbles.

Cyclic AMP Analysis

The PE cells were isolated from the choroid by gently forcing fluid through a Pasteur pipette over the tissue surface. The process was begun along the cut edge, which passed through the optic disk. In some cases, the cells were freed by gently nudging the cells with the tip of the pipette. Once this process was completed, the cells were pipetted into a petri dish containing standard Ringer's plus the appropriate amount of PDE inhibitor. After a 5-min incubation period, ~1 ml of fluid containing the isolated cells was drained off, placed in a chilled test tube, frozen, and lyophilized. In other experiments, the PE-choroid was first placed in the Ringer's containing PDE inhibitors and then the PE cells were isolated. Both procedures gave the same results.

Cyclic nucleotides were assayed following the procedure described by Farber and Lolley (1982). Briefly, lyophilized tissue was homogenized in 0.4 ml of 0.1 N HCl and a 0.1-ml aliquot was removed for the measurement of protein by the method of Lowry et al. (1951). The rest of the homogenate was then boiled and centrifuged at 2,500 *g* for 10 min, and the supernatant fraction was separated and diluted with 50 mM sodium acetate buffer, pH 6.2. Dilutions were 1:3 for control samples and 1:5 for those containing PDE inhibitors. Three serial dilutions of each PE and choroidal sample were assayed in duplicate. The cyclic nucleotides were acetylated before radioimmunoassay. The succinyltyrosine [¹²⁵I]methyl ester derivatives of cAMP and cGMP and the antibodies against

these cyclic nucleotides were purchased from New England Nuclear, Boston, MA. Assay variation within a single sample was ~5–10%. The incubation mixture contained, in order of addition, 100 μ l of cyclic nucleotide standards or sample, 5 μ l of a mixture of acetic anhydride and methylamine, 100 μ l (~10,000 cpm) of 125 I-labeled antigen, which includes 1% normal rabbit serum, and 100 μ l of antiserum complex in 50 mM sodium acetate buffer, pH 6.2. Tubes were incubated overnight at 4°C, and after addition of 1 ml of cold buffer, they were centrifuged at 3,000 *g* for 30 min. The supernatant fractions were aspirated and the precipitates were counted for 1 min in a gamma counter. After subtraction of nonspecific binding, total counts per minute/bound in the standards were plotted against increasing femtomoles of standard added and the cyclic nucleotide concentration in the tissue samples was read from the linear plot. These values, corrected for the appropriate dilution factors, were divided by the protein content and expressed in picomoles per milligram of protein.

Electrophysiology

The chamber design and the techniques used for dissecting the tissue and mounting it between two Lucite plates were identical to those used in previous studies (Miller and Steinberg, 1977*a*; Miller et al., 1978). The tissue was mounted as a membrane separating two separate fluid compartments, which were continuously perfused with the control bathing solution. The compositions of these two solutions could be controlled separately. In both the apical and basal chambers, a calomel electrode made electrical contact with the perfusion solution via a Ringer-agar bridge. The TEP was recorded (apical side positive) differentially between the two calomel electrodes. Membrane potentials from RPE cells were recorded with micropipette electrodes, with respect to either the apical or basal calomel electrode. When referred to the apical calomel electrode, the voltage measured was the apical membrane potential, V_A , and when referred to the basal calomel electrode, the voltage measured was the basal membrane potential, V_B .

The experiments can be analyzed in terms of an equivalent circuit that was previously found to describe passive and active electrical properties of the apical and basal membranes of the isolated frog RPE (Miller and Steinberg, 1977*b*; Miller et al., 1978; Oakley et al., 1978). In this circuit (Fig. 1) the apical membrane is modeled as a resistance, R_A , in series with a battery, V'_A . Similarly, the basal membrane is modeled as a resistance, R_B , in series with a battery, V'_B . The PE membrane resistances are shunted by a resistor, R_S , which represents the parallel combination of the resistance of damaged cells at the edge of the tissue and the paracellular resistance across the extracellular junctional complexes. When both membranes are perfused with the standard Ringer's solution, a steady current, i , flows through the circuit in the counterclockwise direction, since V'_A is greater in magnitude than V'_B (Miller and Steinberg, 1977*a*). This current hyperpolarizes the basal membrane and depolarizes the apical membrane. Thus, the potentials recorded by an intracellular microelectrode, V_A and V_B , differ in absolute magnitude from the membrane batteries, V'_A and V'_B , respectively. At all times the TEP is equal to $V_A - V_B$.

A change in either membrane battery will alter the shunt current i and therefore change the membrane polarization at the opposite membrane. For example, a depolarization of the basal membrane will, in turn, depolarize the apical membrane by increasing i . Using the passive model of the RPE, it can be shown that for all changes in V'_B ,

$$\frac{\Delta V_A}{\Delta V_B} = \frac{R_A}{R_A + R_S} \leq 1, \quad (1)$$

where ΔV_A and ΔV_B are the microelectrode-recorded changes in apical and basal membrane potential, and it is assumed that all the resistances remain constant. This equation predicts that the change in membrane potential will always be larger across the basal

membrane. The inequality holds even in the face of large (factor of 2) changes in the resistances. However, the equation does fail when the electrogenic Na-K pump, located at the apical membrane, is stimulated (Oakley et al., 1978). In that case, the depolarizing current shunted to the apical membrane is augmented by the Na-K pump-generated hyperpolarization of the apical membrane such that $\Delta V_A/\Delta V_B$ is significantly greater than 1. This information will be used to help analyze the data in Fig. 6.

There are two additional measurements, resistance ratios, which can be used to help determine the cAMP-induced changes in tissue resistance. They are obtained by passing constant transepithelial current pulses (6 μ A) across the tissue and monitoring the

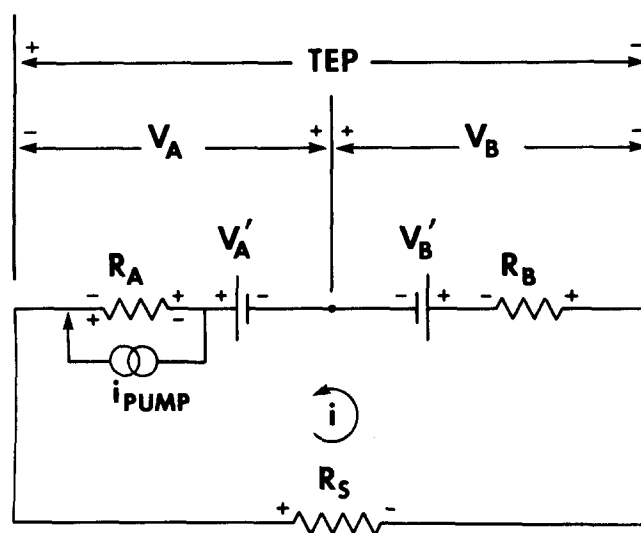


FIGURE 1. Equivalent circuit for the RPE. The apical and basal membranes are each represented by a resistor (R) in series with a battery (V). Subscripts A and B denote the apical and basal membranes, respectively. These membranes are shunted by a resistor (R_s) as described in the text. A steady constant current (i) flows through the circuit because of the difference between V_A and V_B . The electrogenic pump on the apical membrane is modeled as a current source (i_{pump}). The steady potential across the tissue is called the transepithelial potential (TEP).

appropriate voltage response, ΔV . These ratios are defined as follows:

$$\frac{1}{R_t} = \frac{1}{R_A + R_B} + \frac{1}{R_s} \text{ and } a = \frac{\Delta V_A}{\Delta V_B} = \frac{R_A}{R_B}. \quad (2)$$

For a given pulse of current, R_t is determined from the change in TEP and a from the ratio of apical to basal membrane voltage drops.

RESULTS

Effects of cAMP on Ion Transport under Short-Circuit Conditions

CHLORIDE TRANSPORT Fig. 2 illustrates the effect of cAMP and the PDE inhibitor IBMX on the unidirectional fluxes of ^{36}Cl . The data in this figure were

obtained from paired tissues of the same eye. In the lower panel, the open circles represent the retina-to-choroid fluxes in the direction of active transport. The closed circles represent the "back" fluxes in the choroid-to-retina direction. The solid line in the lower panel is the mean steady state flux in the choroid-to-retina

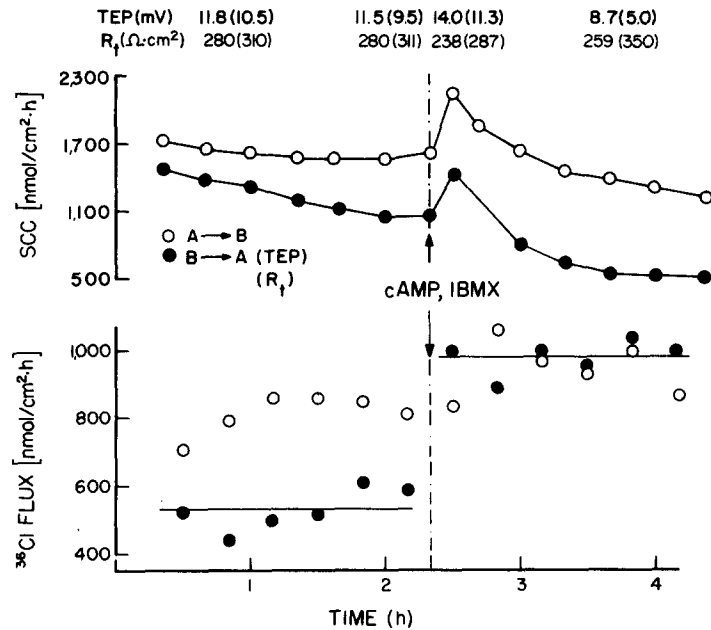


FIGURE 2. Effect of cAMP on the unidirectional ^{36}Cl fluxes. As shown in the lower panel, ^{36}Cl was added either to the apical solution or the basal solution at $t = 0$, and the level of radioactivity was sampled at 20-min intervals from the "cold" solution. The closed symbols represent the choroid-to-retina unidirectional fluxes (J_B) and the open symbols represent the retina-to-choroid unidirectional fluxes (J_A), the direction of active transport. Both tissues were from the same eye. Just before the addition of cAMP and IBMX, the values of R_t and TEP were $280 \Omega \cdot \text{cm}^2$ and 11.5 mV, respectively, for the preparation in which J_A was measured and $315 \Omega \cdot \text{cm}^2$ and 9.5 mV, respectively, for the preparation in which J_B was measured. The steady state rate of active transport ($J_A - J_B$) was $\sim 300 \text{ nmol/cm}^2 \cdot \text{h}$ before the addition of cAMP and IBMX. Cyclic AMP (1 mM) and IBMX (0.5 mM) were added to the solutions bathing the apical and basal membranes at $t = 2 \text{ h}$, 20 min. The upper panel shows that this caused a large transient increase in SCC (and TEP) and a significant decrease in R_t : $42 \Omega \cdot \text{cm}^2$ in one tissue (open symbols) and $28 \Omega \cdot \text{cm}^2$ in the other tissue (closed symbols). Cyclic AMP and IBMX practically abolished the active Cl transport.

direction. In these experiments, steady state fluxes were obtained within an hour after the tracer was added to the solutions bathing the apical (retinal) or basal (choroidal) side of the tissue.

The upper panel in this figure shows the SCC, expressed in units of nanomoles per square centimeter per hour. Indicated at the top of the upper panel are the

TEP and R_t at various times. The values in parentheses are the voltages and resistances for the choroid-to-retina data (B \rightarrow A) and the adjacent numbers give the voltages and resistances for the A \rightarrow B flux experiment.

The active Cl transport in Fig. 2 is the difference between the retina-to-choroid flux (open symbols) and the choroid-to-retina flux (closed symbols). This net ^{36}Cl flux is $\approx 300 \text{ nmol/cm}^2 \cdot \text{h}$ before the addition of cAMP and IBMX. At $t = 2 \text{ h}$ and 20 min, cAMP (1 mM) and IBMX (0.5 mM) were added to the solutions bathing both sides of the tissue. This caused an immediate rise in the choroid-to-retina flux, from 550 to 1,000 $\text{nmol/cm}^2 \cdot \text{h}$. In contrast, the unidirectional flux in the direction of active transport, retina to choroid, was practically unaltered. This shows that exogenously applied cAMP and IBMX can significantly reduce active ^{36}Cl transport across the RPE by increasing the "back" flux.

TABLE I
Cyclic AMP-induced Changes in ^{36}Cl Transport

Retina to choroid (A \rightarrow B)	Control	cAMP	Difference
Unidirectional flux ($\mu\text{eq/cm}^2 \cdot \text{h}$)	1.08 \pm 0.08 (20)	0.99 \pm 0.07 (20)	-0.09 \pm 0.05 (steady state)
SCC ($\mu\text{eq/cm}^2 \cdot \text{h}$)	1.56 \pm 0.11	—	+0.51 \pm 0.05* (peak)
R_t ($\Omega \cdot \text{cm}^2$)	280 \pm 12.6	—	-34.3 \pm 4.2* (peak)
Choroid to retina (B \rightarrow A)	Control	cAMP	Difference
Unidirectional flux ($\mu\text{eq/cm}^2 \cdot \text{h}$)	0.81 \pm 0.07 (34)	1.20 \pm 0.09 (34)	+0.39 \pm 0.06* (steady state)
SCC ($\mu\text{eq/cm}^2 \cdot \text{h}$)	1.32 \pm 0.08	—	+0.41 \pm 0.04* (peak)
R_t ($\Omega \cdot \text{cm}^2$)	291 \pm 9.8	—	-40.6 \pm 3.5* (peak)
Net flux ($\mu\text{eq/cm}^2 \cdot \text{h}$)	0.27 (A \rightarrow B) [†]	0.21 (B \rightarrow A)	0.48

The values in each column are means \pm SEM. In columns 2 and 3, the numbers in parentheses refer to the number of tissues. The magnitude and direction of the net flux, before and after cAMP, is given in columns 2 and 3 (bottom). This active transport is the algebraic difference between the retina-to-choroid and choroid-to-retina unidirectional fluxes. The magnitude of net Cl transport under control conditions (column 2, bottom) is significantly different from zero ($^{\dagger}P = 0.014$; unpaired t test). After cAMP (column 3), the magnitude of net Cl transport is not significantly different from zero ($P = 0.12$). The cAMP-induced changes in resistance, SCC, and choroid-to-retina flux are all statistically significant (* $P < 0.001$; paired t test).

These substances also cause an increase in TEP and SCC, along with a decrease in R_t (Figs. 2–6). In Fig. 2, the peak changes in SCC, TEP, and R_t occur 8 min after the addition of cAMP and IBMX. The mean values of these peak changes are summarized in Tables I–III. Figs. 2 and 3 also show that the rise in the choroid-to-retina ^{36}Cl flux coincides with the increase in SCC, but remains elevated even after the current falls.

Table I is a summary of the results of 54 experiments in which unidirectional fluxes of ^{36}Cl were measured before and after the addition of cAMP. 12 of these experiments were carried out using paired tissues (Figs. 2 and 3) from the same eye. One purpose of these experiments was to compare the effects of cAMP, dbcAMP, and IBMX on the unidirectional fluxes. The results were practically identical whether cAMP or dbcAMP was added alone or in combination with IBMX to the solutions bathing one or both sides of the tissue. All of these

experiments were therefore pooled together in Table I. In 10 experiments (not shown), IBMX was added to the solutions bathing one or both sides of the tissue. The changes in TEP, R_t , and flux were in the same direction as those obtained with cAMP or dbcAMP, but smaller in magnitude by ~50%.

The data summarized in Table I substantiate the results shown in Figs. 2 and 3. Cyclic AMP caused an increase of the mean steady state choroid-to-retina flux in each of the 34 experiments (range: 0.10–1.4 $\mu\text{eq}/\text{cm}^2\cdot\text{h}$). Under control conditions in the short-circuit state, there was a significant net ^{36}Cl flux in the retina-to-choroid direction of 0.27 $\mu\text{eq}/\text{cm}^2\cdot\text{h}$ (column 2, bottom, $P = 0.014$), which was completely inhibited by cAMP (column 3). Cyclic AMP apparently reversed the direction of net flux from absorption to secretion, but the magnitude of this net flux is not significantly different from zero ($P = 0.12$, unpaired t test).

The cAMP-induced changes in resistance, SCC, and unidirectional flux are shown in column 4 ("Difference"). The changes in steady state flux were obtained within 20–40 min, while the electrical changes peaked in ~5 min and then returned toward their control values (Figs. 2–5).

CYCLIC AMP STIMULATION FROM THE APICAL OR BASAL SOLUTION The physiological responses induced by the exogenous application of cAMP may be different when the nucleotide is added to the solution bathing the apical or basal side of the tissue. This could happen because of significant differences in membrane permeability or because the choroid imposes a significant diffusion barrier between the bulk solution and the basal membrane (Miller and Steinberg, 1977a; Oakley et al., 1978).

Fig. 3 illustrates the responses to a single-sided addition of cAMP. In the experiment illustrated in Fig. 3A, the solution composition change was made on the apical side of the tissue and in part B the change was made only on the basal side. In both cases the changes in SCC, TEP, R_t , and unidirectional flux were very similar, but the time to peak of the SCC was much shorter, ≈ 5 min, when the composition change was made on the apical compared with the basal (≈ 20 min) side of the tissue. This was a consistent finding for all the tissues studied; the average time to peak was 6.25 ± 0.95 min ($n = 14$) for the apical solution change and 17.5 ± 0.83 min ($n = 11$) for the basal solution change. This difference is most probably due to a diffusion delay through the large unstirred layer created by the choroid (Miller and Steinberg, 1977b).

In 25 experiments of the type described in Fig. 3, we increased the cAMP concentration to 1 mM in the apical or basal solutions and compared the magnitude of the changes in the unidirectional flux, SCC, and R_t . Although the mean changes in flux and SCC were larger when cAMP was added to the apical side, the differences were not statistically significant. Therefore, it seems likely that cAMP has approximately equal access to the RPE cells through the apical and basal membranes.

SODIUM TRANSPORT We next examined the effect of cAMP on unidirectional ^{22}Na fluxes. In Fig. 4 (same format as Fig. 2), the net ^{22}Na flux before the addition of cAMP was ≈ 500 nmol/ $\text{cm}^2\cdot\text{h}$ and the addition of cAMP to the solution bathing the apical membrane caused an immediate rise in the choroid-to-retina flux (closed circles). This is the direction of active Na transport. As in

the case of Cl transport, there was little or no change in the retina-to-choroid ^{22}Na fluxes (open circles). In this case, the net active ^{22}Na flux increased from ≈ 500 to $1,000$ $\text{nmol}/\text{cm}^2 \cdot \text{h}$. A comparison of Figs. 2 and 4 shows that cAMP increased net ^{22}Na flux and decreased net ^{36}Cl flux across the RPE. In both

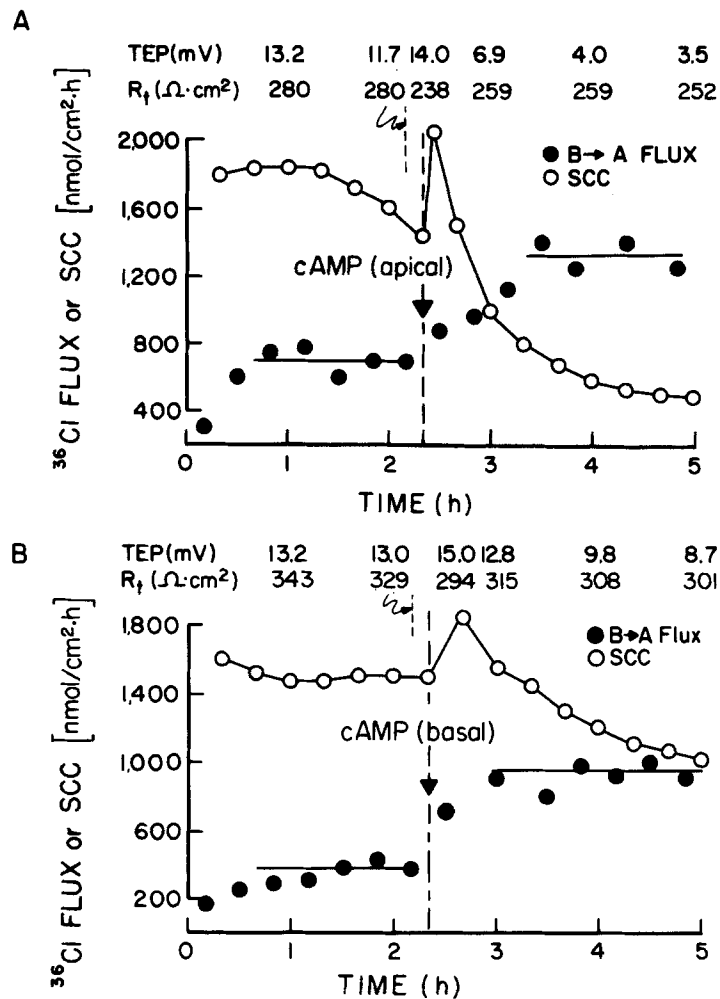


FIGURE 3. Effect of cAMP on choroid-to-retina ^{36}Cl flux. In *A*, cAMP (1 mM) was added to the solution bathing the apical membrane. In *B*, the cAMP was added to the solution bathing the basal membrane. Other conditions were the same as in Fig. 2.

cases, the choroid-to-retina unidirectional flux increased, while the retina-to-choroid flux was relatively unaffected. For Na, the increase took place in the direction of active transport; for Cl, the increase occurred in the direction opposite to active transport.

Table II summarizes 28 paired experiments in which we measured the cAMP-

induced changes in ^{22}Na unidirectional fluxes. As with ^{36}Cl , these changes were practically identical whether one added cAMP or dbcAMP with or without IBMX to the solutions bathing one or both sides of the tissue. Column 2 (bottom) corroborates what has been previously shown (Miller and Steinberg, 1977*b*): that there is a significant active transport of ^{22}Na in the choroid-to-retina direction under control conditions. A comparison of the results in columns 2 and 3 shows that cAMP approximately doubled the active transport of Na in the choroid-to-retina direction.

POTASSIUM TRANSPORT It was previously demonstrated that in the PE there are Na-K pumps located on the apical but not on the basal membrane.

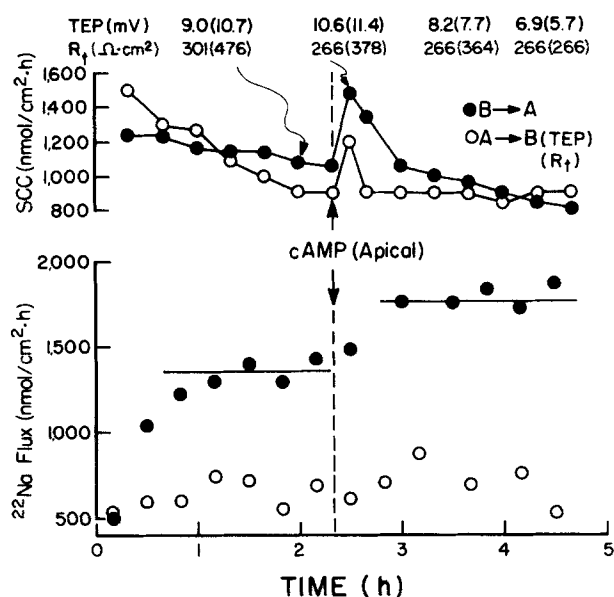


FIGURE 4. Effect of cAMP on unidirectional ^{22}Na fluxes. Cyclic AMP (1 mM) was added to the solution bathing the apical membrane. Other conditions were the same as in Fig. 2. The net active Na transport, $\approx 500 \text{ nmol/cm}^2 \cdot \text{h}$, was approximately doubled after the addition of cAMP.

These pumps are responsible for the active transepithelial transport of Na and K in the short-circuit state (Miller and Steinberg, 1977*b*, 1982; Miller et al., 1978; Oakley et al., 1978; Riley et al., 1978; Ostwald and Steinberg, 1980; Bok, 1982). In the short-circuit state, with $[\text{K}]_o = 2 \text{ mM}$ on both sides of the tissue, there is a net transport of K in the retina-to-choroid direction. This net flux, which is 30–50 $\text{nmol/cm}^2 \cdot \text{h}$, accounts for $\sim 2.5\%$ of the SCC (Miller and Steinberg, 1979, 1982). Previously, it was shown that ^{86}Rb and ^{42}K are equivalent tracers for studying the movements of K across the RPE (Miller and Steinberg, 1982). Therefore, in the present study, ^{86}Rb was used to trace the movements of K.

Fig. 5 is a representative experiment in which we measured the effect of cAMP on active K transport. In this experiment, carried out using paired tissues from

the same eye, the net flux before the application of cAMP was ≈ 30 nmol/cm²·h. At $t = 2$ h and 20 min, the cAMP concentration in the solution bathing the apical membrane was elevated to 1 mM. This caused a rise in SCC and TEP (3–4 mV) and a decrease in R_t ($84 \Omega \cdot \text{cm}^2$) in both tissues. The active K transport increased by a factor of 4, from 30 to 125 nmol/cm²·h. Most of this change occurred as a result of the cAMP-induced increase in the retina-to-choroid unidirectional flux (open circles). The choroid-to-retina flux (closed circles) was not appreciably altered by cAMP.

Table III is a summary of 14 such experiments, all carried out on paired tissues from the same or contralateral eye. Column 2 (bottom) shows that the net flux before cAMP was 50 nmol/cm²·h and that cAMP increased this rate by more than a factor of 3, to 160 nmol/cm²·h.

TABLE II
Cyclic AMP-induced Change in ²²Na Transport

Retina to choroid (A → B)	Control	cAMP	Difference
Unidirectional flux ($\mu\text{eq}/\text{cm}^2 \cdot \text{h}$)	1.28±0.08 (14)	1.35±0.08 (14)	+0.07±0.04 (steady state)
SCC ($\mu\text{eq}/\text{cm}^2 \cdot \text{h}$)	1.52±0.09	—	+0.40±0.06* (peak)
R_t ($\Omega \cdot \text{cm}^2$)	312±20	—	-47±9.1* (peak)
Choroid to retina (B → A)	Control	cAMP	Difference
Unidirectional flux ($\mu\text{eq}/\text{cm}^2 \cdot \text{h}$)	1.60±0.13 (14)	1.95±0.10 (14)	+0.35±0.06* (steady state)
SCC ($\mu\text{eq}/\text{cm}^2 \cdot \text{h}$)	1.51±0.07	—	+0.50±0.04* (peak)
R_t ($\Omega \cdot \text{cm}^2$)	288±13	—	-42±4.2* (peak)
Net flux ($\mu\text{eq}/\text{cm}^2 \cdot \text{h}$)	0.32 (B → A) [‡]	0.60 (B → A) [‡]	0.28

The net Na flux, before and after cAMP, is in the choroid-to-retina direction (columns 2 and 3, bottom). In both cases, the magnitude of this net flux is significantly different from zero ([‡] $P = 0.03$; [‡] $P < 0.001$; unpaired t test). The cAMP-induced changes in resistance, SCC, and choroid-to-retina unidirectional flux are all statistically significant ($*P < 0.001$; paired t test).

In sum, the addition of cAMP to either of the solutions bathing the RPE significantly altered the active transport of Cl, Na, and K. Active Cl transport was completely inhibited and may have been reversed, while active Na and K transport were stimulated by cAMP. In each case, only one of the unidirectional fluxes was significantly altered; the Na and Cl fluxes were increased in the secretory (choroid-to-retina) direction and the K unidirectional flux was increased in the absorptive (retina-to-choroid) direction.

Effects of cAMP on Membrane Voltage and Resistance

The above data show that exogenous cAMP produces an increase in TEP and a decrease in R_t . It is not possible to determine from these experiments whether these changes took place at the apical and/or basal membrane; nor can one eliminate the possibility of a resistance change in the shunt pathway. Therefore, additional experiments were undertaken to help specify the locus of these electrical changes.

In this series of experiments, microelectrodes were placed in the PE cells to monitor apical and basal membrane potentials, R_t , and the ratio of apical to basal

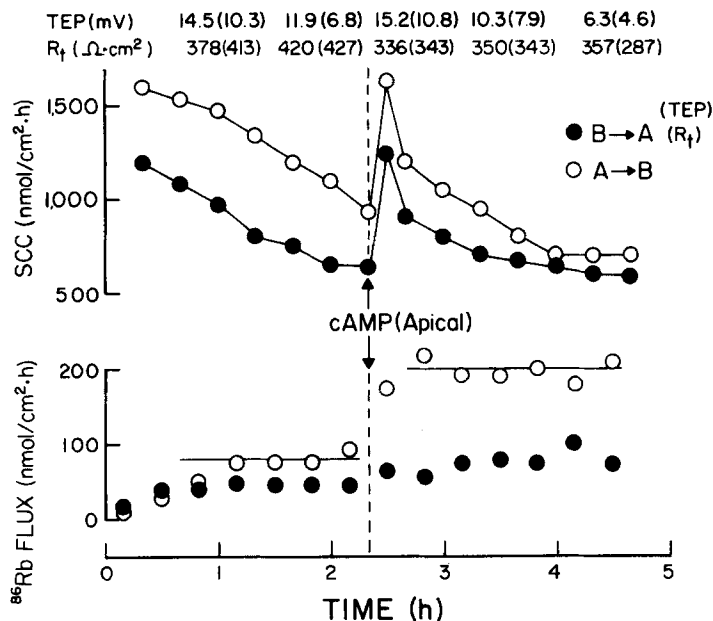


FIGURE 5. Effect of cAMP on K transport. Cyclic AMP (1 mM) was added to the solution bathing the apical membrane. Other conditions were the same as in Fig. 2. ^{86}Rb was used to trace the movements of K across the epithelium (see text). Cyclic AMP increased the rate of net K absorption, $\approx 30 \text{ nmol/cm}^2 \cdot \text{h}$, by a factor of more than 4.

membrane resistance, $R_A/R_B = a$. The latter two quantities were obtained by passing 6- μA current pulses across the tissue with a microelectrode in the cell (see Methods). These parameters and the TEP were recorded before and after 1 mM cAMP was added to the solution bathing the apical membrane. The results

TABLE III
Cyclic AMP-induced Changes in K (^{86}Rb) Transport

Retina to choroid (A \rightarrow B)	Control	cAMP	Difference
Unidirectional flux ($\mu\text{eq/cm}^2 \cdot \text{h}$)	0.08 ± 0.02 (7)	0.23 ± 0.04 (7)	$+0.15 \pm 0.02^*$ (steady state)
SCC ($\mu\text{eq/cm}^2 \cdot \text{h}$)	1.12 ± 0.08	—	$+0.53 \pm 0.07^*$ (peak)
R_t ($\Omega \cdot \text{cm}^2$)	315 ± 36	—	$-60 \pm 7.7^*$ (peak)
Choroid to retina (B \rightarrow A)	Control	cAMP	Difference
Unidirectional flux ($\mu\text{eq/cm}^2 \cdot \text{h}$)	0.03 ± 0.005 (7)	0.07 ± 0.01 (7)	$+0.04 \pm 0.008^*$ (steady state)
SCC ($\mu\text{eq/cm}^2 \cdot \text{h}$)	1.33 ± 0.16	—	$+0.54 \pm 0.03^*$ (peak)
R_t ($\Omega \cdot \text{cm}^2$)	308 ± 28	—	$-63 \pm 12^*$ (peak)
Net flux ($\mu\text{eq/cm}^2 \cdot \text{h}$)	0.05 (A \rightarrow B) [‡]	0.16 (A \rightarrow B) [§]	0.11

The active K transport is in the retina-to-choroid direction before and after cAMP (columns 2 and 3, bottom). In both cases, the magnitude of this flux difference is significantly different from zero ($^{\ddagger}P = 0.02$; $^{\S}P < 0.001$; unpaired t test). The cAMP-induced changes in resistance, SCC, and unidirectional flux are all statistically significant ($^*P < 0.001$; paired t test).

from one such experiment are shown in Fig. 6. This record was obtained by Jean-Paul Vincent working in this laboratory.

The center panel of Fig. 6 shows the cAMP-induced changes in transepithelial potential (*A*) and basal membrane potential (*B*). At $t = 0$, the apical solution concentration of cAMP was elevated from 0 to 1 mM. It took ~ 1 min for the cAMP to alter the concentration of the bulk solution and penetrate through the unstirred layer to the apical membrane (Miller et al., 1978). In this period, there may have been some baseline drift in the records. After ~ 1 min, the TEP rose sharply and there was a concomitant depolarization of the basal membrane

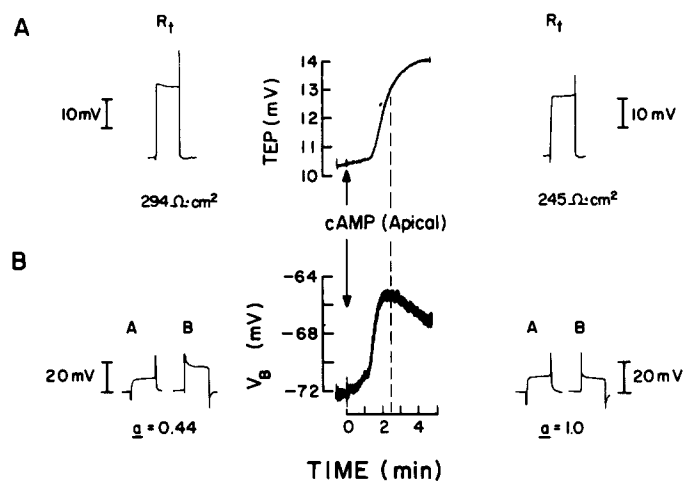


FIGURE 6. Cyclic AMP-induced changes in resistance and voltage. Panel *A* (middle) shows the time course of the TEP change (apical side positive) that occurred as a result of adding 1 mM cAMP to the solution bathing the apical membrane. The transepithelial resistance was measured 1 min before the addition of cAMP and at 5 min after the addition of cAMP. Panel *B* (middle) shows the time course of the basal membrane potential change (cell negative) that occurred after the apical addition of cAMP. The ratio of apical to basal membrane resistance (a) was measured just before the addition of cAMP and at ~ 5 min after its addition to the apical solution.

potential. The apical membrane also must have depolarized, since the magnitude of the basal membrane depolarization exceeded the increase in TEP and $\Delta \text{TEP} = \Delta V_A - \Delta V_B$ (see Methods). This net depolarization between 1 and 2 min could have been due to the “passive” shunting of current from the basal to the apical membrane via the shunt, R_s (see Fig. 1), or it could have been due to the combined effect of shunting and a cAMP-induced potential change at the apical membrane.

At approximately $t = 2$ min, the basal membrane potential leveled off but the TEP continued to rise. This could only occur if the apical membrane were hyperpolarizing. At $t = 2$ min, the basal membrane began to repolarize and since the TEP continued to increase during this period, this means that the apical membrane was also hyperpolarizing. In Fig. 6 the magnitude of the apical

membrane hyperpolarization between $t = 2$ and 4 min is $\Delta V_A = \Delta TEP + \Delta V_B \approx 3.0$ mV.

Therefore, the initial effect of cAMP ($0 \leq t \leq 2$ min) is to depolarize the basal membrane and, possibly, to hyperpolarize the apical membrane. The apical membrane hyperpolarization may be masked in the first 2 min by the depolarization shunted from the basal to the apical membrane (Methods). In any case, cAMP does cause a hyperpolarization of the apical membrane at $t \geq 2$ min.

The magnitudes of R_t and a were measured just before the addition of cAMP ($t = 1$ min) and at $t = 5$ min. Fig. 6A shows that cAMP caused a decrease in R_t from 294 to 245 $\Omega \cdot \text{cm}^2$, which is comparable to the results shown in Figs. 2–5 and the data summarized in Tables I–III. The a value more than doubled from 0.44 to 1.0 (Fig. 6B).

In five cells from four tissues, cAMP increased the TEP by 2.8 ± 0.2 mV (mean \pm SD) and depolarized the basal membrane by 4.7 ± 0.03 mV. In these tissues, cAMP decreased the average R_t ($288 \pm 24 \Omega \cdot \text{cm}^2$) by $41.2 \pm 8.4 \Omega \cdot \text{cm}^2$. Cyclic AMP also increased a from 0.59 ± 0.06 to 1.06 ± 0.04 . If one assumes (Discussion) that R_s is unaffected by cAMP (Eq. 2), then these resistance changes imply that cAMP decreased the basal membrane conductance. These data do not, however, eliminate the possibility of concomitant changes in apical membrane resistance. The membrane mechanism(s) underlying these voltage and resistance changes is under investigation.

cAMP Levels in the RPE

The physiological responses summarized in Figs. 2–5 and Tables I–III are presumably mediated by a rise in the cellular cAMP levels. Therefore, one should be able to observe a correlation between the changes in cellular cAMP levels and the changes in ion transport. This notion was tested in a series of experiments using the PDE inhibitors IBMX and SQ65442.

In the first series of experiments, the isolated PE-choroid was mounted in the same chamber that was used to measure the changes in unidirectional fluxes. The PDE inhibitors IBMX (0.5 mM) and SQ65442 (1 mM) were then added to the solutions bathing both sides of the tissue. These inhibitors increased the SCC and decreased R_t , but the changes were smaller, by $\approx 50\%$, than the responses produced with cAMP in the bathing solutions. The unidirectional fluxes were also altered in a manner qualitatively similar to that shown in Table I–III, but these changes were small and not precise.

Once the electrical response was obtained, the tissues were quickly removed from the chamber, punched out, and prepared for cyclic nucleotide analysis (Methods). In control tissues (unstimulated), the cAMP level was 12 ± 2.1 pmol/mg protein (mean \pm SEM, $n = 7$), and when the PE-choroid preparation was exposed to IBMX and SQ65442, the value rose to 30 ± 2.9 pmol/mg protein ($n = 17$). This result was corroborated in another series of experiments in which the average cAMP level was 5.5 ± 1.2 pmol/mg protein ($n = 5$) in the control tissues and 39.1 ± 13.1 pmol/mg protein ($n = 5$) in tissues treated with IBMX. In both sets of experiments, the differences between the means are significant ($P < 0.001$). In these experiments, the measured cAMP level might have included

a significant contribution from the choroid. This was important to verify since epithelial salt and water transport are presumably determined by the cellular and not the choroidal part of the tissue.

In the next series of experiments, the epithelial cells were scraped off the choroid. The choroidal tissue was then bathed in Ringer's containing IBMX and SQ65442. In the control choroidal tissues, the cAMP level was 19.6 ± 2.7 pmol/mg protein ($n = 10$), and in the PDE inhibitor-exposed tissues, the value was 69.1 ± 8.7 pmol/mg protein ($n = 10$). The difference between the means is

TABLE IV
Cyclic Nucleotide Levels

Experimental protocol	Control	PDE inhibited
	<i>pmol/mg protein</i>	<i>pmol/mg protein</i>
(1) One experiment per retina cAMP	6.0 ± 0.8 ($n = 6$)	$24.5 \pm 1.6^*$ ($n = 6$)
(2) Two experiments per retina cAMP	7.5 ± 1.1	$38.6 \pm 3.4^*$
cGMP	3.1 ± 0.6 ($n = 5$)	$6.4 \pm 0.9^*$ ($n = 5$)
(3) Two experiments per retina (DMSO omitted) cAMP	5.1 ± 0.6 ($n = 6$)	$29.6 \pm 2.1^*$ ($n = 6$)
(4) Two experiments per retina (DMSO omitted) cGMP	—	6.4 ± 0.7 ($n = 10$)
(5) Two experiments per retina	—	55.5 ± 8.6 ($n = 8$) [‡] 956.3 ± 194.2 ($n = 5$) [§]

In all of the experiments shown in rows 1–5, the cyclic nucleotide levels were measured using isolated PE cells relatively free of choroidal contamination (see Methods). In row 1, the Ringer's bathing the treated cells contained IBMX (0.5 mM) and SQ65442 (1 mM) dissolved in 0.4% DMSO. In the experiments summarized in rows 2–4, the PE-choroid from a single retina was divided in two halves; one half was used as the control, and the other half was treated with PDE inhibitors. In the experiments summarized in row 2, the cAMP and cGMP levels were both measured in each experiment. In rows 3 and 4, DMSO was omitted from the Ringer's since it may also elevate cAMP levels. In each case, cAMP levels were significantly increased above control ($*P < 0.001$). In row 4, the cGMP levels were measured in the presence of 0.5 mM IBMX. In row 5, the cAMP levels were measured in the presence of 0.5 mM IBMX (‡) and 0.5 mM IBMX plus forskolin (§). Forskolin was dissolved in 0.475% ethanol (placed in the control and treated solutions).

significant ($P < 0.001$). These data indicate that the choroid contains a significant amount of PDE.

In order to measure the cellular cAMP levels relatively free of choroidal contamination, individual PE cells or small sheets of cells were isolated (Methods). In these experiments, two different protocols were used and the results are shown in Table IV. Each of the 12 experiments summarized in row 1 was carried out using PE-choroid from single retinae. The control and treated tissues came from different eyes of the same frog or from different frogs. In each case, the PE-choroid was incubated for 5 min either in normal Ringer's or in normal Ringer's plus PDE inhibitors. The cells were then isolated and analyzed for cAMP content. The PDE inhibitors produced an approximately fourfold increase in cellular cAMP.

This finding was corroborated using a different protocol shown in rows 2–5 of Table IV. In these experiments, the PE-choroid from a single retina was divided in two halves; one half was used as a control, and the other half was treated with the PDE inhibitors. The cells from both halves were then isolated and prepared for cyclic nucleotide analysis. In some experiments, this procedure was reversed; that is, the cells were first isolated and then treated with PDE inhibitors. This was done to test the possibility that some cAMP accumulated in the choroid and then diffused into the PE cells. In 10 comparison experiments, however, the cAMP levels were virtually identical using both procedures. The data summarized in rows 2 and 3 show that the PDE inhibitors produced a fivefold increase in cellular cAMP. The cGMP levels, in the same set of tissues, were also measured. Row 2 shows that the PDE inhibitors IBMX and SQ65442 had no appreciable effect on RPE cGMP levels. This finding was corroborated in another series of experiments summarized in row 4. In these experiments, the cGMP levels were measured in the presence of 0.5 mM IBMX. This treatment did not appreciably alter the cGMP level above that found in the control Ringer's without IBMX (row 2, column 2).

In another set of experiments (Table IV, row 5), the cAMP levels in the PE cells were increased by a factor of ~18 using forskolin, 10^{-4} M, which stimulates adenylate cyclase in other systems (Seamon and Daley, 1981). In these experiments, the solutions bathing the control half of the tissue contained 0.5 mM IBMX, while the experimental half contained IBMX plus forskolin.

The results summarized in Table IV strongly suggest that the biochemical machinery responsible for cAMP elevation remained intact, even after the PE cells were removed from the choroid. Furthermore, the results as a whole demonstrate that increasing cAMP levels in the pigment epithelial cells can mediate significant changes in ion transport across the epithelium. The quantitative relationship between cAMP levels and changes in transepithelial ion transport remains to be determined.

DISCUSSION

In the PE, the cellular levels of cAMP can be increased by the exogenous application of cAMP or PDE inhibitors, and by substances such as forskolin, which in other systems stimulate adenylate cyclase (Seamon and Daley, 1981). The increase of extracellular cAMP significantly alters the transepithelial transport of ions (this paper) and fluid (companion paper). The present study shows that: (a) The cAMP levels in the PE cell are significantly increased (a factor of 5–7) by the PDE inhibitors IBMX and SQ65442 and by forskolin. (b) In the short-circuit state, cAMP stimulates the active Na and K transport across the RPE and inhibits the active Cl transport. (c) It does this in a specific way, by increasing the secretion of NaCl and the absorption of K. The unidirectional fluxes of Na and Cl in the retina-to-choroid (absorptive) direction and K in the choroid-to-retina (secretory) direction are relatively unaffected by elevations in the extracellular levels of cAMP. (d) Increasing cAMP in the PE cells transiently increases the SCC (TEP) and decreases R_t . (e) The increase in TEP is due to a cAMP-mediated depolarization of the basal membrane, which is followed by,

and perhaps also accompanied by, a hyperpolarization of the apical membrane. (f) Cyclic AMP increases the apparent ratio of cell membrane resistances, R_A/R_B .

cAMP and Active Ion Transport

CHLORIDE In a previous study it was demonstrated that the active transport of Cl, but not Na, is seasonally dependent (Miller and Steinberg, 1977a). In this regard, it is worth noting that almost all of the chloride experiments summarized in Table I, column 2, were carried out in October, November, and December of succeeding years. In the present study, the average net chloride flux, $0.27 \mu\text{eq}/\text{cm}^2 \cdot \text{h}$, is very similar to that obtained in a comparable time period (November and December) of the previous study ($0.36 \mu\text{eq}/\text{cm}^2 \cdot \text{h}$). We also found during the course of the present experiments that the cAMP-induced increase in the $B \rightarrow A$ flux was very small or absent during the summer months. This might have occurred because the PE cells of the summer frogs already have an elevated cAMP level, which cannot be significantly elevated further by the exogenous supply of cAMP. This hypothesis would also explain the relative and variable reduction of active Cl transport that is observed during the summer months (Miller and Steinberg, 1977b; unpublished observations).

The data summarized in Table I include 12 experiments using matched tissues from the same eye (for example, see Fig. 2). In these experiments, the net flux before cAMP ranged from 0.25 to $0.50 \mu\text{eq}/\text{cm}^2 \cdot \text{h}$. In all of these experiments, the effect of cAMP was to abolish the net Cl absorption by increasing the "back" flux of ^{36}Cl in the choroid-to-retina direction (Fig. 2).

SODIUM AND POTASSIUM It was previously demonstrated that the Na-K pump, located on the apical membrane of this epithelium, is responsible for the active transepithelial transport of Na and K (Miller and Steinberg, 1982). Figs. 4 and 5 and Tables II and III show that cAMP stimulated the active secretion of Na and the active absorption of K.

There are at least two ways in which this stimulation could occur. The data in some systems suggest that cyclic nucleotides can directly alter Na-K ATPase activity (Silva et al., 1979; Stewart and Sen, 1981). In other systems, cyclic nucleotides modulate the permeability of an ionic channel, probably via the phosphorylation of plasma membrane proteins (Klyce and Wong, 1977; Schofeniels and Dandrifosse, 1980; Orloff, 1981; Kandel and Schwartz, 1982). In the latter case, the stimulation of the Na pump might occur indirectly via an alteration in extracellular chemical activity. The present experiments do not allow us to differentiate between these two possibilities.

It seems unlikely that the cAMP-induced changes in resistance and voltage (Fig. 6) are produced by a change in R_s alone. The microelectrode experiments suggest that there was a significant resistance change in the cellular pathway, since the apparent voltage divider ratio increased from ≈ 0.6 to 1.06 (Results) and the basolateral membrane depolarized in the first few minutes of the response. These changes are consistent with a cAMP-induced conductance change at the basolateral membrane. In addition, cAMP decreased R_t by $\approx 40 \Omega \cdot \text{cm}^2$ (Results). If this decrease were due only to a decrease in R_s , then the

equivalent circuit that describes this system (Miller and Steinberg, 1977a; Oakley et al., 1978) would predict that the basolateral membrane would hyperpolarize in response to cAMP, contrary to what is observed.

Conversely, if one assumes that the main effect(s) of cAMP is in the cellular pathway and, in particular, at the basolateral membrane, then one can use Eq. 2 and the observed changes in R_t and a to calculate R_A and R_S . Inserting the control and cAMP-induced mean values for R_t and a (see Results) into Eq. 2, one obtains for R_A and R_S 246 and 508 $\Omega \cdot \text{cm}^2$, respectively. These values of R_A and R_S can be compared with those obtained previously from an entirely different class of microelectrode experiments not involving cAMP (Miller and Steinberg, 1977a, Table I[c]). In the previous study, we obtained $R_A = 250 \pm 18 \Omega \cdot \text{cm}^2$ (mean \pm SEM, $n = 14$) and $R_S = 447 \pm 32 \Omega \cdot \text{cm}^2$ ($n = 14$). This agreement is practically perfect and is consistent with the notion that the main effect of cAMP is on the basolateral conductance.¹ If, for example, this conductance increase occurred in a passive Na channel, this would explain the initial basal membrane depolarization. It might also lead to an increase in extracellular Na activity, which would stimulate the electrogenic Na pump and produce the observed apical membrane hyperpolarization ($t > 2$ min). It is also possible that the apical membrane hyperpolarization is a direct result of cAMP stimulation of the Na,K-ATPase (Silva et al., 1979). Of course, these observations and calculations do not exclude the possibility of cAMP-induced changes in apical membrane and/or shunt resistances.

APPARENT BICARBONATE TRANSPORT It has been shown previously (Miller and Steinberg, 1977b, 1982; Steinberg and Miller, 1979) and confirmed in the present study (Tables I–III, column 2) that in the short-circuit state the RPE actively secretes Na and absorbs K and Cl and that the SCC is much larger than the algebraic sum of the net fluxes of these ions. That is, $\text{SCC} \gg J_{\text{net}}^{\text{Na}} (\text{B} \rightarrow \text{A}) + J_{\text{net}}^{\text{K}} (\text{A} \rightarrow \text{B}) + J_{\text{net}}^{\text{Cl}} (\text{A} \rightarrow \text{B})$. It was also shown that net Ca and Mg fluxes are very small (5–10 nmol/cm²·h) and cannot account for the difference. Qualitatively similar results have been obtained in the toad RPE (Lasansky and DeFisch, 1966). All of these data were obtained under control conditions without cAMP.

The lack of equality between the SCC and the algebraic sum of the measured net fluxes (Na, K, Cl, Mg, and Ca) could be due to the active absorption of an anion, $J_{\text{net}} (\text{A} \rightarrow \text{B})$, or secretion of a cation, $J_{\text{net}} (\text{B} \rightarrow \text{A})$. Given the composition of the Ringer's, the anion must be bicarbonate and the cation must be hydrogen. Because there is a net absorption of fluid across this epithelium (Hughes et al., 1984), the most likely possibility is that the tissue actively absorbs bicarbonate.

¹ This conclusion can be further tested by assuming that cAMP does alter apical membrane conductance (assuming R_S is constant), for example, by $\pm 10\%$. In this case, Eq. 2 yields control values of $R_A = 334 \Omega \cdot \text{cm}^2$ (+10%) or $158 \Omega \cdot \text{cm}^2$ (–10%) and $R_S = 424 \Omega \cdot \text{cm}^2$ (+10%) or $891 \Omega \cdot \text{cm}^2$ (–10%). Three out of four of these values are significantly different from those obtained in the previous microelectrode experiments not involving cAMP (Miller and Steinberg, 1977a, Table I[c]; $R_A = 250 \pm 18 \Omega \cdot \text{cm}^2$ and $R_S = 447 \pm 32 \Omega \cdot \text{cm}^2$). Therefore, it seems likely that any cAMP-induced change in R_A was less than or equal to $\pm 10\%$. If most of the tissue resistance change occurred at the basal membrane, one can use the ratio of the a values obtained before and after cAMP (0.59 ± 0.12 and 1.06 ± 0.08 , respectively) to estimate that cAMP increased the basal membrane conductance by $\approx 80\%$.

An analysis of the open-circuit fluxes (see Hughes et al., 1984) leads to the same conclusion.

The rate of bicarbonate transport across the RPE can be estimated from the difference between the mean SCC and the algebraic sum of all the net fluxes. Inspection of Tables I–III (column 2) shows that the algebraic sum of the net fluxes is $0.54 \mu\text{eq}/\text{cm}^2 \cdot \text{h}$, while the mean SCC varies between 1.12 and $1.54 \mu\text{eq}/\text{cm}^2 \cdot \text{h}$. Therefore, the rate of active bicarbonate transport is estimated to be $0.60\text{--}1.0 \mu\text{eq}/\text{cm}^2 \cdot \text{h}$. The difference between the SCC and the sum of the net fluxes obtained after the addition of cAMP is more difficult to quantify. This difficulty stems from the complexity of the membrane response(s) to cAMP (Fig. 6), which does not permit us to estimate the steady state SCC.

Although these measurements allow us to estimate the rate of HCO_3^- transport, they shed no light on the underlying membrane mechanisms. In previous electrophysiological studies, it was found that the apical membrane has an "apparent" bicarbonate conductance that is relatively high, $T_{\text{HCO}_3^-} \approx 0.39$ (Miller and Steinberg, 1977a). The voltage responses of the apical membrane to step changes in $[\text{HCO}_3^-]_o$ could be due to a HCO_3^- diffusion potential and/or to an electrogenic pump mechanism. In contrast, it was determined that the voltage response of the basal membrane to step changes in $[\text{HCO}_3^-]_o$ is not measurably different from zero. Therefore, bicarbonate probably moves across this membrane by some neutral exchange or co-transport system.

Cyclic Nucleotide Levels in the RPE

The cAMP levels in the PE cells can be elevated in several different ways, and in each case there is a concomitant change in transepithelial transport and electrical properties. The cAMP levels in the cells are increased by increasing the exogenous concentration of cAMP, PDE inhibitors (Table IV), and dopamine or forskolin (S. Miller and D. Farber, manuscript in preparation), which are both potent stimulators of adenylate cyclase in a variety of intact cells and membranes (Creese et al., 1981; Seamon and Daley, 1981). Except for dopamine and the PDE inhibitor IBMX, all of these substances significantly increase the secretion of NaCl, increase TEP, and decrease R_i ; the changes in the ion fluxes and the electrical parameters induced by dopamine and IBMX are relatively small and more difficult to quantify.

In addition to its inhibitory action on cAMP-PDE, IBMX can, in some systems, significantly increase the extracellular levels of cGMP by inhibiting cGMP-PDE. In the RPE, however, IBMX has no appreciable effect on cGMP levels (Table IV).

In a two-year period, we observed some variability in the PE cAMP response to PDE inhibition. This response is sometimes larger (never smaller) than that shown in Table IV (column 3). In one series of experiments, the control level of cAMP, $11.7 \pm 2.0 \text{ pmol}/\text{mg}$ protein ($n = 6$), was elevated to $84.0 \pm 8.5 \text{ pmol}/\text{mg}$ protein ($n = 6$) after the addition of PDE inhibitors to the bathing solution. This increase in cAMP level exceeds that shown in Table IV by a significant amount and the reason for this difference is not known. One possible source of variability stems from the large variations in steroid hormone levels that have

been demonstrated in bullfrog plasma. These levels are significantly altered by stress (handling), they undergo significant seasonal variations, and depend on sex (Licht et al., 1983).

In some systems there is a very tight coupling between Ca and cAMP (Rasmussen, 1981). However, in the PE, increasing the exogenous levels of cAMP has no effect on net Ca transport across the epithelium, but loading the cells with Ca, via the ionophore A123187, does cause a significant increase in cellular cAMP levels (S. Miller and D. Farber, manuscript in preparation). Although it seems most likely that all of the changes described in the present work are mediated by an increase in cell cAMP, a role for Ca cannot be ruled out.

We are grateful to B. Hughes, T. E. Machen, L. Reuss, and E. Wright for their helpful comments during the preparation of this manuscript. We also wish to thank J. Chow, A. Halio, D. Joseph, and D. W. Souza for their expert technical assistance.

This work was supported by research grants EY 02205 (S.M.) and EY 02651 (D.F.), Research Career Development Award EY 144 (D.F.), and Core Center Grant EY 03176.

Received for publication 15 November 1983 and in revised form 13 January 1984.

REFERENCES

- Besharse, J. C., D. A. Dunis, and B. Burnside. 1982. Effects of cyclic adenosine 3',5'-monophosphate on photoreceptor disc shedding and retinomotor movement. *J. Gen. Physiol.* 79:775-790.
- Bok, D. 1982. Autoradiographic studies on the polarity of plasma membrane receptors in retinal pigment epithelial cells. *In* IVth International Symposium on the Structure of the Eye. J. Hollyfield, editor. Elsevier/North-Holland, New York. 247-256.
- Brown, B. L., and M. H. Makman. 1972. Stimulation by dopamine of adenylate cyclase in retinal homogenates and of adenosine 3',5'-cyclic monophosphate formation in intact retina. *Proc. Natl. Acad. Sci. USA.* 69:539-543.
- Burnside, B., M. Evans, T. R. Fletcher, and G. J. Chader. 1982. Induction of dark-adaptive retinomotor movement (cell elongation) in teleost retinal cones by cyclic adenosine 3',5'-monophosphate. *J. Gen. Physiol.* 79:759-774.
- Capovilla, M., L. Cervetto, and V. Torre. 1980. Effects of changing external potassium and chloride concentrations on the photoresponses of *Bufo bufo* rods. *J. Physiol. (Lond.)* 307:529-551.
- Creese, I., D. R. Sibley, S. Lett, and M. Hamblin. 1981. Dopamine receptors: subtypes, localization and regulation. *Fed. Proc.* 40:147-152.
- Farber, D. B., and R. N. Lolley. 1982. Measurement of cyclic nucleotides in retina. *Methods Enzymol.* 81:551-556.
- Farber, D. B., D. W. Souza, D. G. Chase, and R. N. Lolley. 1981. Cyclic nucleotides of cone-dominant retinas: reduction of cyclic AMP levels by light and by cone degeneration. *Invest. Ophthalmol. Visual Sci.* 20:24-31.
- Gass, J. D. M. 1977. Stereoscopic Atlas of Macular Diseases. C. V. Mosby Co., St. Louis, MO. 19-38.
- Hudspeth, A. J., and A. G. Yee. 1973. The intracellular junctional complexes of retinal pigment epithelia. *Invest. Ophthalmol. Visual Sci.* 12:354-365.
- Hughes, B. A., S. S. Miller, and T. E. Machen. 1984. Effects of cyclic AMP on fluid absorption

- and ion transport across frog retinal pigment epithelium. Measurements in the open-circuit state. *J. Gen. Physiol.* 83:875-899.
- Kandel, E. R., and J. H. Schwartz. 1982. Molecular biology of learning: modulation of transmitter release. *Science (Wash. DC)*. 218:433-442.
- Klyce, S. D., and R. K. S. Wong. 1977. Site and mode of adrenalin action on chloride transport across the rabbit corneal epithelium. *J. Physiol. (Lond.)*. 266:777-779.
- Lasansky, A., and F. W. DeFisch. 1966. Potential, current, and ionic fluxes across the isolated retinal pigment epithelium and choroid. *J. Gen. Physiol.* 49:913-924.
- Licht, P., B. R. McCreery, R. Barnes, and R. Pang. 1983. Seasonal and stress related changes in plasma gonadotropins, sex steroids and corticosterone in the bullfrog, *Rana catesbeiana*. *Gen. Comp. Endocrinol.* 50:124-145.
- Lowry, O. H., N. J. Rosebrough, A. L. Farr, and R. J. Randall. 1951. Protein measurement with the Folin phenol reagent. *J. Biol. Chem.* 193:265-275.
- Miller, S. S. 1982. Cyclic AMP modulated transport in retinal pigment epithelium. *ARVO Abstr.* 13.
- Miller, S. S., and D. B. Farber. 1981. Cyclic nucleotides and NaCl transport in frog pigment epithelium. *ARVO Abstr.* 194.
- Miller, S. S., B. A. Hughes, and T. E. Machen. 1982. Fluid transport across retinal pigment epithelium is inhibited by cyclic AMP. *Proc. Natl. Acad. Sci. USA.* 79:2111-2115.
- Miller, S. S., and R. H. Steinberg. 1977a. Passive ionic properties of frog retinal pigment epithelium. *J. Membr. Biol.* 36:337-372.
- Miller, S. S., and R. H. Steinberg. 1977b. Active transport of ions across frog retinal pigment epithelium. *Exp. Eye Res.* 25:235-248.
- Miller, S. S., and R. H. Steinberg. 1979. Potassium modulation of taurine transport across the frog retinal pigment epithelium. *J. Gen. Physiol.* 74:237-259.
- Miller, S. S., and R. H. Steinberg. 1982. Potassium transport across the frog retinal pigment epithelium. *J. Membr. Biol.* 67:199-209.
- Miller, S. S., R. H. Steinberg, and B. Oakley II. 1978. The electrogenic sodium pump of the frog retinal pigment epithelium. *J. Membr. Biol.* 44:259-279.
- Miller, W. H. 1981. Molecular mechanisms of photoreceptor transduction. *Curr. Top. Membr. Transp.* 15:1-452.
- Nilsson, S. E. G. 1964. An electron microscopic classification of the retinal receptors of the leopard frog (*Rana pipiens*). *J. Ultrastruct. Res.* 10:390-416.
- Oakley, B., II. 1977. Potassium and the photoreceptor-dependent pigment epithelial hyperpolarization. *J. Gen. Physiol.* 70:405-425.
- Oakley, B., II, S. S. Miller, and R. H. Steinberg. 1978. Effect of intracellular potassium upon the electrogenic pump of frog retinal pigment epithelium. *J. Membr. Biol.* 44:281-307.
- Orloff, J. 1981. Regulation of cyclic GMP (AMP) metabolism. In *Water Transport Across Epithelia*. Alfred Benzon Symposium 15. H. H. Ussing, N. Bindslev, N. A. Lassen, and O. Sten-Knudsen, editors. Munksgaard, Copenhagen. 393-403.
- Orloff, J., and J. S. Handler. 1962. The similarity of effects of vasopressin, 3'-5' AMP (cyclic AMP) and theophylline on the toad bladder. *J. Clin. Invest.* 41:702-709.
- Ostwald, T., and R. H. Steinberg. 1980. Localization of frog retinal pigment epithelium (Na, K)-ATPase. *Exp. Eye Res.* 31:351-360.
- Porter, K. R., and E. Yamada. 1960. Studies on the endoplasmic reticulum. V. Its form and differentiation in pigment epithelial cells of the frog retina. *J. Biophys. Biochem. Cytol.* 8:181-205.

- Rasmussen, H. 1981. Calcium and cAMP as Synarchic Messengers. John Wiley & Sons, New York. 1-370.
- Riley, M. V., B. S. Winkler, J. Benner, and E. M. Yates. 1978. ATPase activities in retinal pigment epithelium and choroid. *Exp. Eye Res.* 26:445-455.
- Schoffeniels, E., and G. Dandriofosse. 1980. Protein phosphorylation and sodium conductance in nerve membrane. *Proc. Natl. Acad. Sci. USA.* 77:812-816.
- Seamon, K., and J. W. Daley. 1981. Activation of adenylate cyclase by the diterpene forskolin does not require the guanine nucleotide regulatory protein. *J. Biol. Chem.* 256:9799-9871.
- Silva, P., J. Staff, and F. H. Epstein. 1979. Indirect evidence for enhancement of Na-K-ATPase activity with stimulation of rectal gland secretion. *Am. J. Physiol.* 237:F468-F472.
- Steinberg, R. H. 1973. Scanning electron microscopy of the bullfrog's retina and pigment epithelium. *Z. Zellforsch. Mikrosk. Anat.* 143:451-463.
- Steinberg, R. H., and S. S. Miller. 1979. Transport and membrane properties of the retinal pigment epithelium. *In The Retinal Pigment Epithelium.* K. M. Zinn and M. F. Marmor, editors. Harvard University Press, Cambridge, MA. 205-225.
- Steinberg, R. H., B. Oakley II, and G. Niemeyer. 1980. Light evoked changes in $[K^+]$ in the retina of the intact cat eye. *J. Neurophysiol.* 44:897-921.
- Steinberg, R. H., and I. Wood. 1979. The relationship of the retinal pigment epithelium to photoreceptor outer segments in the human retina. *In The Retinal Pigment Epithelium.* K. M. Zinn and M. F. Marmor, editors. Harvard University Press, Cambridge, MA. 32-44.
- Stewart, D. J., and A. K. Sen. 1981. Role of cyclic GMP in cholinergic activation of Na-K pump in duck salt gland. *Am. J. Physiol.* 240:C207-C214.
- Van Buskirk, R., and J. E. Dowling. 1981. Isolated horizontal cells from carp retina demonstrate dopamine-dependent accumulation of cyclic AMP. *Proc. Natl. Acad. Sci. USA.* 78:7825-7829.
- Zauberman, H. 1979. Adhesive forces between the retinal pigment epithelium and sensory retina. *In The Retinal Pigment Epithelium.* K. M. Zinn and M. F. Marmor, editors. Harvard University Press, Cambridge, MA. 192-204.